ANIMAL CELLS AND SYSTEMS
2020, VOL. 24, NO. 6, 311–320
https://doi.org/10.1080/19768354.2020.1837951

Taylor & Francis
Taylor & Francis Group

Microfluidic approaches for *Caenorhabditis elegans* research

Erel Levine[a] and Kyung Suk Lee[b]

[a]Department of Bioengineering, Northeastern University, Boston, MA, USA; [b]Department of Physics Education, Kongju National University, Gongju, South Korea

ABSTRACT
In the last decade, microfluidic methods have proven to be powerful tools for *Caenorhabditis elegans* research, offering advanced manipulation of worms and precise control of experimental conditions. The advantages of microfluidic chips include their capability of immobilization, automated sorting, and longitudinal measurement, and more. In this review, we focus on control components that are widely used in the design of microfluidic devices, and discuss their functions and working principles that enable advanced manipulation on a chip. Understanding these components will ease the onboarding of researchers inexperienced with microfluidics and help them bring the power of microfluidics to new applications.

ARTICLE HISTORY
Received 16 September 2020
Accepted 5 October 2020

KEYWORDS
C. elegans; microfluidics; immobilization; sorting; automation

Introduction

Caenorhabditis elegans is a small soil nematode with many advantages as a research model organism. It is easy to cultivate with a reproduction cycle of a few days, and its short lifespan of a few weeks makes lifelong studies manageable. The body is transparent, which is ideal for imaging *in vivo*. Moreover, its whole genome sequence, complete cell lineage of development, and neuronal connectivity map are all available. Because of many advantages including the abovementioned, researchers have employed this organism to study various aspects of biology, such as genetics, neurobiology, and aging (Midkiff and San-Miguel 2019).

In the last 20 years, the need for miniaturization of analytical techniques, precise control of experimental conditions, and automation for high throughput assays accelerated the advent of microfluidics in biological studies (Kamili and Lu 2018). *C. elegans* research has also benefitted from the introduction of these techniques, and microfluidic chips have been applied to address a broad variety of questions in worm biology (Muthaiyan Shanmugam and Subhra Santra 2016).

Most microfluidic chips used in studying worms are made of polydimethylsiloxane (PDMS), an air-permeable material that allows long-term on-chip experiments with living animals. The PDMS layer for microfluidic devices is manufactured using a mold fabricated by photolithography, and therefore the micro-structures on a chip can be custom-designed at a spatial resolution of 10 μm (Midkiff and San-Miguel 2019), namely at the scale of the worm diameter.

Combined with a software-controlled microscope and programmable pumps regulating flow and pressure, microfluidics enables advanced control of experimental conditions and fine manipulation of worms. The followings are some of the advantages offered by adapting microfluidics for *C. elegans*. (1) Worms can be immobilized for high-resolution applications, including imaging at subcellular resolution, optogenetic manipulation (Stirman et al. 2010; Hwang et al. 2016), or fully automated femtosecond laser axotomy (Gokce et al. 2014). (2) Flow-controlled microfluidic devices can be used for automated sorting of worms with high throughput. Applications include sorting of eggs for age-synchronization (Sofela et al. 2018), sorting progenies for automatic counting (Li et al. 2015), sorting adults and larvae by their developmental stages (Casadevall i Solvas et al. 2011; Ai et al. 2014), and sorting mutants based on motor abnormalities (Rezai et al. 2012) and fluorescent reporters (Yan et al. 2014). (3) Some microfluidic chips offer capability of longitudinal imaging of individuals for studying development (Hulme et al. 2010; Cornaglia et al. 2015; Keil et al. 2017), aging (Li et al. 2015), and stress response (Banse et al. 2019). (4) Holding worms in a microfluidic chamber allows precise and fast control of their environment (Chronis et al. 2007; Albrecht and Bargmann 2011; Schrödel et al. 2013; Kopito and Levine 2014; Lee et al. 2016). (5) Finally, there are a number of interesting experiments available on-chip such as electrotaxis (Rezai et al. 2012), pharyngeal activity (Lockery et al. 2012;

CONTACT Kyung Suk Lee leeks@kongju.ac.kr

Scholz et al. 2016), mechanical stimuli (Cho, Porto, et al. 2017), and acoustic manipulation (Ahmed et al. 2016) studies.

Applications of microfluidics to study worms have been reviewed extensively in recent years (Muthaiyan Shanmugam and Subhra Santra 2016; Kamili and Lu 2018), highlighting biological findings from novel microfluidic chips (Youssef et al. 2019), as well as the potential of these new assays (Cho, Zhao, et al. 2017; Cornaglia et al. 2017; Midkiff and San-Miguel 2019). In this review we focus instead on control components that are frequently used in many of these chips to address some basic requirements. We discuss their function, design, and implementation, and examine how they are combined together. Our aim is to facilitate onboarding of researchers who are interested in adapting microfluidics in their applications.

Immobilization

Standard experiments in the lab involve cultivating worms on solid media plates. Experiments that require high-resolution imaging at subcellular resolution inevitably demand transfer of individual worms to another imaging platform, such as an agar pad on a microscope slide. In contrast, experiments in which worms are held in a microfluidic device enable *in situ* high-resolution imaging without having to anesthetize them or manually transfer them to another platform. This increases the throughput of the experiments and reduces the burden of manual labour.

A simple strategy for immobilizing worms is to trap them in microstructures that surround them (Figure 1(A)). A tapered channel is a simple but useful design where worms are pushed by flow into the channel where they are eventually trapped. This simple component has been used in many applications (Hulme et al. 2007, 2010; Shi et al. 2010; Lee et al. 2014; Mondal et al. 2016). The same principle of trapping by flow has also been applied to embryos to generate 'embryo incubators' (Figure 1(B)) for long-term imaging of the embryonic development (Cornaglia et al. 2015). Efficient immobilization, however, has adverse effects on worm health and physiology, leading researchers to consider different types of trapping channels for durable imaging (Kopito and Levine 2014; Li et al. 2015).

Side suction is another widely used strategy for short-term immobilization of worms in microfluidic devices (Figure 1(C,D)), where worms are pushed toward the sidewall of the chamber by a suction flow. In this scheme, the sidewall exhibits an array of microstructures that hold the worm while allowing a free flowthrough of the buffer. Suction is maintained by withdrawing the buffer through the microstructures to an outlet port connected to a negative pressure (Rohde et al. 2007; Chung et al. 2008; Hu et al. 2013; Gokce et al. 2014).

Two-layer design enables more advanced control in a microfluidic device. Here the main layer that holds the animals is separated from the control chamber by a thin layer of dimethylsiloxane polymer. The control chamber can expand into the main layer under high pressure. This can be used to create 'pressure valves' (Figure 2(B)), which in a layout trap the worm into a small confinement. Such pressure-controlled valves have been employed extensively in microfluidic systems, where researchers can program multiple states of action of their microfluidic chip to execute more advanced tasks (Figure 2(B)) (Rohde et al. 2007; Hulme et al. 2010; Stirman et al. 2010; Ide et al. 2012; Hu et al. 2013; Ai et al. 2014; Hwang et al. 2016; Cho, Porto, et al. 2017).

A double-layer pressurized chamber can also be used to directly press on worms and limit their movement (Figure 2(C)) (Keil et al. 2017). This method, termed compressive immobilization, has also been widely employed in microfluidic chips (Chung et al. 2008; Chokshi et al. 2009; Ma et al. 2009; Gokce et al. 2014; Zhu et al. 2016; Keil et al. 2017), and has allowed *in situ* high-resolution imaging at subcellular resolution (Figure 2(D)) (Keil et al. 2017).

Sorting

Sorting of animals based on observable phenotypes has many applications in worm research, including preparing age-synchronized populations for subsequent experiments, isolating rare mutants in genetic screens, and investigating phenotypic diversity. Using microfluidics for automated sorting eliminates bias, saves time and labour, and avoids the use of sodium hypochlorite for synchronization.

Sorting strategies can be divided into active and passive approaches. Active sorting employs a three-way junction. As shown in Figure 3(A), when a worm enters the junction, flow is directed toward one of two outlets according to the decision made based on imaging the animal before the junction (Yan et al. 2014). Earlier implementations employed pressure valves in a multi-step process that included closing the valves, immobilizing a worm, imaging and making a decision, and opening one of the valves (Rohde et al. 2007; Chung et al. 2008; Zhu et al. 2016). More recent designs use additional control flows (Channels B and C in Figure 3(A)) to perform the sorting (Yan et al. 2014; Aubry et al. 2015). This eliminates the need for a multi-

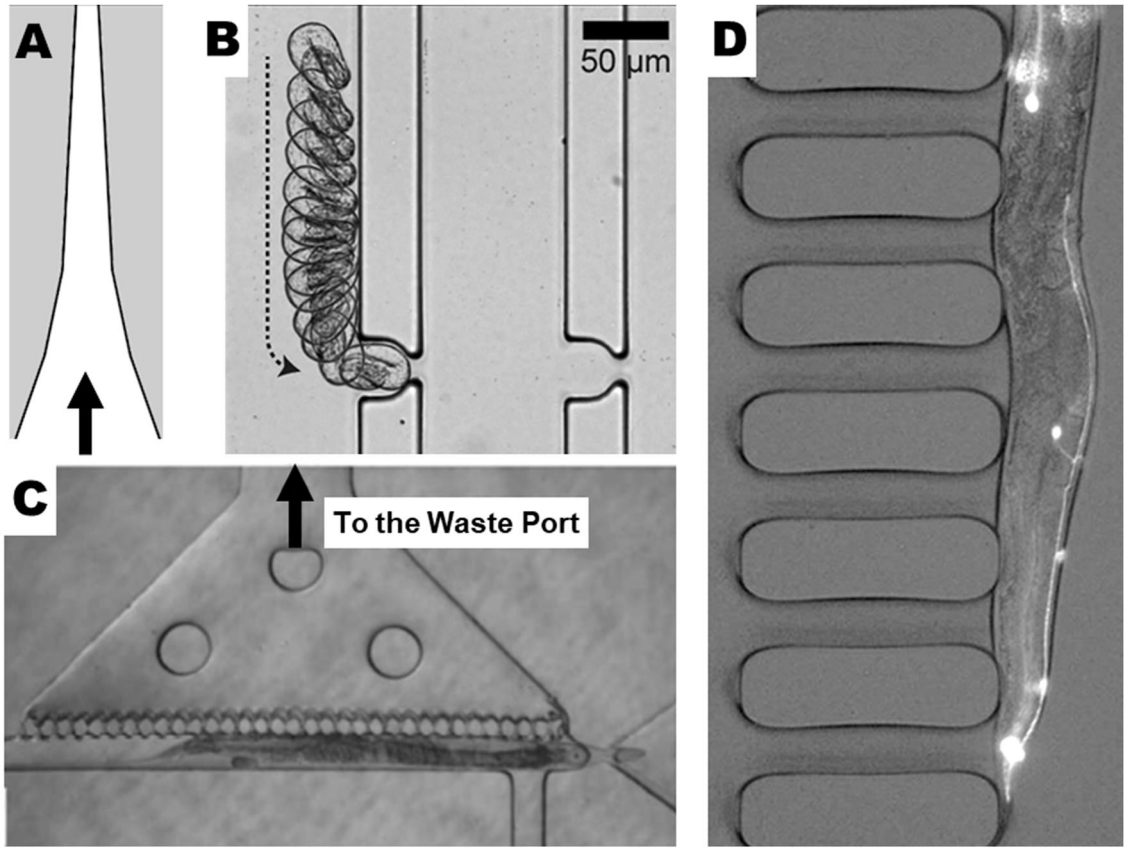

Figure 1. Microstructures for immobilization. (A) Immobilization by a tapered channel. A single worm is pushed by the flow into the channel and is trapped eventually. (B) An embryo stays in an 'embryo incubator' for long-term imaging of embryonic development (Cornaglia et al. 2015). (C) Immobilization of a single worm using side suction for short-term imaging (Hu et al. 2013). The red arrow shows a suction flow to the waste port. (D) A single worm trapped by side suction channels for fluorescence imaging of touch neurons and their processes (Rohde et al. 2007). The images were reproduced from Cornaglia et al. (2015) and Hu et al. (2013) with permission under the terms of the Creative Commons Attribution Non-Commercial License (http://creativecommons.org/licenses/by-nc/4.0), and Rohde et al. (2007) (Copyright (2007) National Academy of Sciences).

layer design, which simplifies the fabrication of the chip, and accelerates sorting by avoiding discrete steps.

Passive sorting techniques usually rely on custom microstructures that lead to a size-dependent difference in worm motility (Figure 3(B–D)). Casadevall i Solvas et al. (2011) demonstrated a 'smart mazes' device (Figure 3 (B)), where a series of main channels are adjoined by interconnecting channels of varying widths. The small width of the main channel hinders crawling of adults and directs them toward one exit, while swimming larvae are flushed through the interconnecting channels of relevant widths. In an alternative design (Han et al. 2012), worms are passed through channels with 'micro-bumps', whose dimensions are adjusted to the undulation frequency of the worms of the desired size. Consequently, such worms reach the outlet efficiently, allowing size-dependent sorting. Similar principles guide a different design (Ai et al. 2014), where the spacing between micro-pillars within the channels affect the worm motility in a size-dependent manner (Lockery et al. 2008). Depending on the dimensions of these microstructures, they could also work only as confinement for worms (Wang et al. 2013).

Finally, a spiral microchannel has been used (Sofela et al. 2018) for high-throughput sorting of eggs from larvae and adults for efficient age-synchronization. This design takes advantage of inertial focusing, a phenomenon in which particles in a laminar pipe flow gather at the annulus of the pipe, facilitating the realization of a very simple, easy-to-adapt technique for separating eggs without bleaching (Figure 3(E)).

Longitudinal imaging

Heterogeneity among individuals can obscure measurements of bulk populations. For example, in a stress response experiment, different individuals could respond to the stimulus at different times even when they are age-synchronized. Those individual traits are lost if only the population average is monitored over

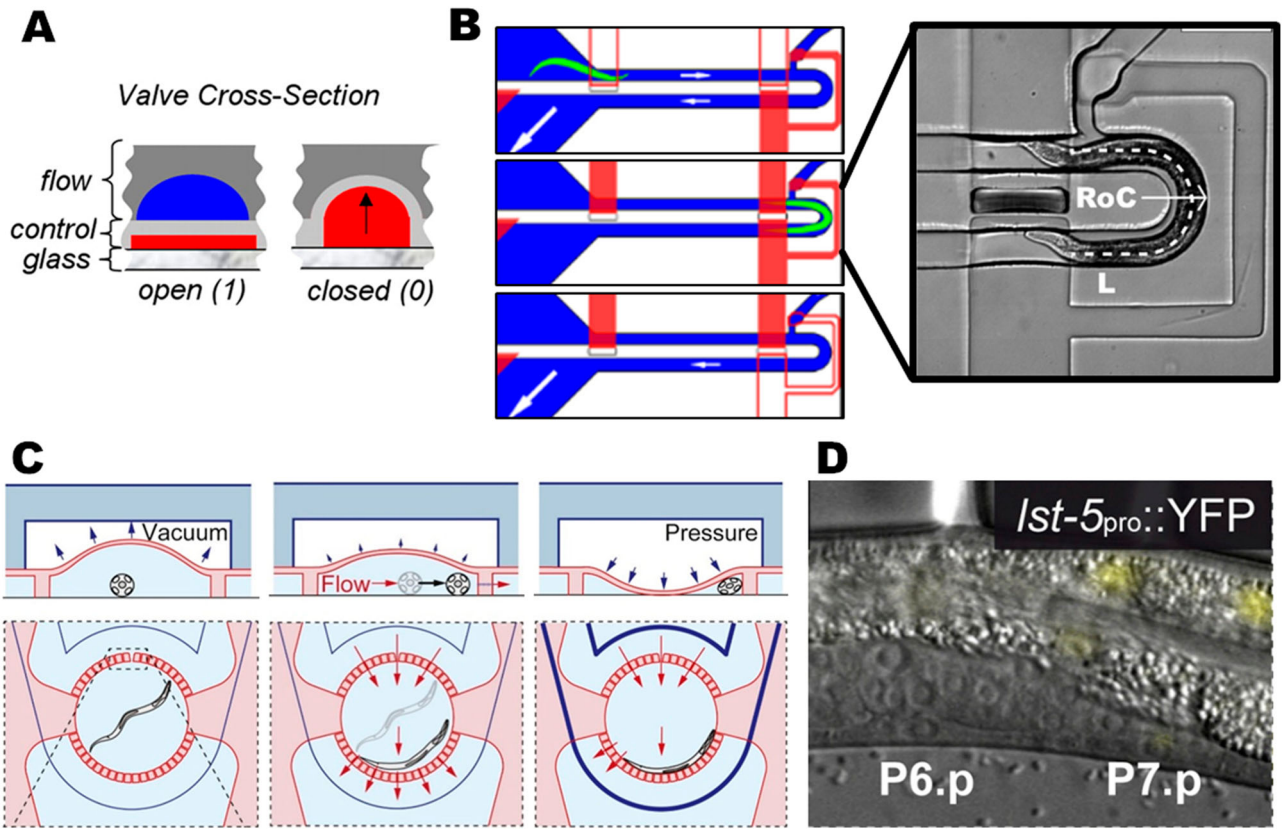

Figure 2. Pressure-controlled chambers. (A) The working principle of pressure valves in microfluidic chips. The main flow chamber and the control layer are coloured in blue and red, respectively. Adapted from Rohde et al. (2007) (Copyright (2007) National Academy of Sciences). (B) Multiple stages of action of a microfluidic chip controlled by pressure valves (Ide et al. 2012). Top: the first two valves are opened to allow the entry of a worm (green). Middle: Once the worm is trapped, all the valves are closed. An actual image of a trapped worm in a flow chamber is shown in an inset. Bottom: the valves on the right are opened to release the worm. Reproduced from Ide et al. (2012) with permission under the terms of the Creative Commons Attribution Non-Commercial License (http://creativecommons.org/licenses/by-nc/4.0) (C) Compressive immobilization. A single worm in a flow chamber is free to move when the pressure in the control chamber is low. To immobilize the worm for imaging, it is pushed to the side by the flow and the pressurized control chamber presses directly on the animal (Keil et al. 2017). (D) High-resolution imaging of an immobilized worm (notch target *lst-5*::YFP during vulval development). The images were adapted from Keil et al. (2017) with permission from Elsevier.

time. Longitudinal experiments, in which individual animals are monitored repeatedly or continuously over time, can therefore be very valuable in studying animal physiology.

Longitudinal measurement of worms freely crawling on solid-media plates is not desirable. Placing single worms on every petri dish is labour-intensive and wastes materials, and monitoring individual worms in a population requires high-frequency imaging and complicated (and often unreliable) image processing.

Many studies have demonstrated longitudinal experiments with microfluidic chips (Figure 4). On a chip, it is very simple to make a confinement of size comparable to that of a single adult worm, of the order of a few mm^2 (300-fold smaller than that of a small petri dish). Imaging in a chip is more suitable for high quality imaging, since it avoids complications that arise from imaging on agar, such as autofluorescence and an uneven surface. A simple design, shown in Figure 4(A) (Li et al. 2015), is based on chambers with two notable features: a tapered worm loading channel and microstructures for flushing out progenies. The tapered channel allows entry of a single worm into the chamber only when it is assisted by a pulse of high pressure, and does not allow it to exit. The microstructures at the bottom prevent adults from passing through them but not small larvae. This chamber is occupied by a single worm that remains confined in the chamber for the duration of an experiment. Hulme *et al.* added a second tapered channel to each chamber to immobilize the confined-but-moving worm for high-resolution imaging (Hulme et al. 2010). This device avoids long-term immobilization, which impacts the worms, by immobilizing worms only when needed for image acquisition. A similar concept is used for other devices that employ compressive immobilization

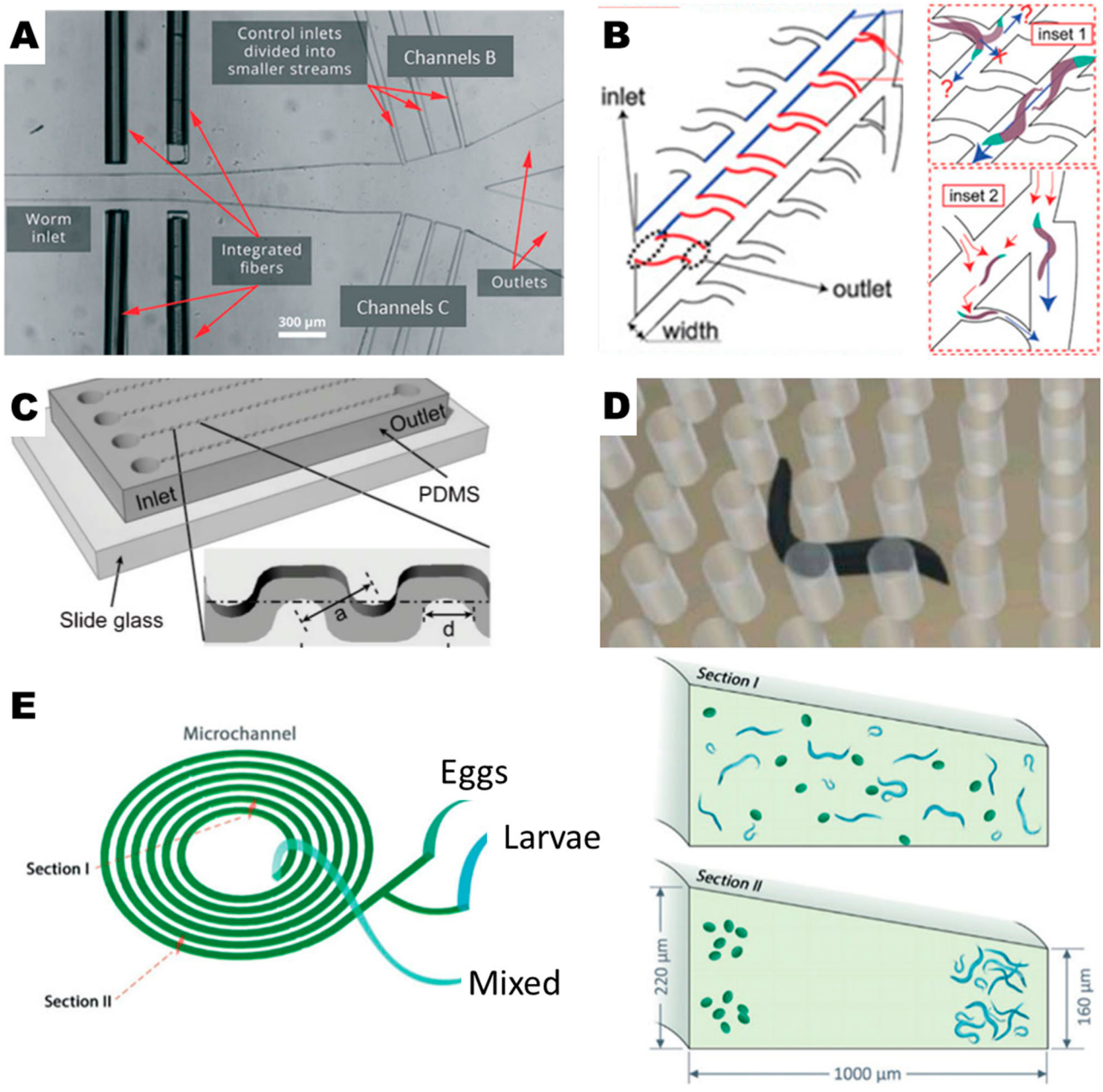

Figure 3. Sorting. (A) Worms entering from the inlet are examined with fluorescence (integrated fibres). Based on the imaging result, they are sent to one of the two outlets by the flows from the control inlets: channels B and C (Yan et al. 2014). (B) A 'smart maze' device by Casadevall i Solvas et al. (2011). A series of main channels (blue, oriented at 45° to the long axis) are adjoined with six interconnecting channels (red) of varying widths in between. Insets show that crawling of adults is hindered and larvae are flushed through the interconnecting channels. (C) A 'micro-bumps' channel developed by Han et al. (2012). (D) Immobilization of worms with an array of micro-pillars (Ai et al. 2014). (E) A spiral microchannel by Sofela et al. (2018). Eggs and larvae are separated while moving through the spiral microchannel. Sections I and II illustrate the mixed and the sorted state. The images were reproduced from Yan et al. (2014), Casadevall i Solvas et al. (2011), Han et al. (2012), Ai et al. (2014), and Sofela et al. (2018) with permission from the Royal Society of Chemistry.

instead of a tapered channel (Figure 2(C)) (Zhu et al. 2016; Keil et al. 2017).

Swimming worms and crawling worms exhibit significantly different gene expression profiles and healthspans (Laranjeiro et al. 2019). Therefore, it is presumed that the results obtained from microfluidic devices where worms crawl rather than swim would be more comparable to those obtained with worms on solid media. Lockery *et al*. introduced such a microfluidic chip, termed 'artificial dirt' (Lockery et al. 2008). As shown in Figure 4(C), in this chip the flow chamber is punctuated by micro-columns arrayed in a hexagonal

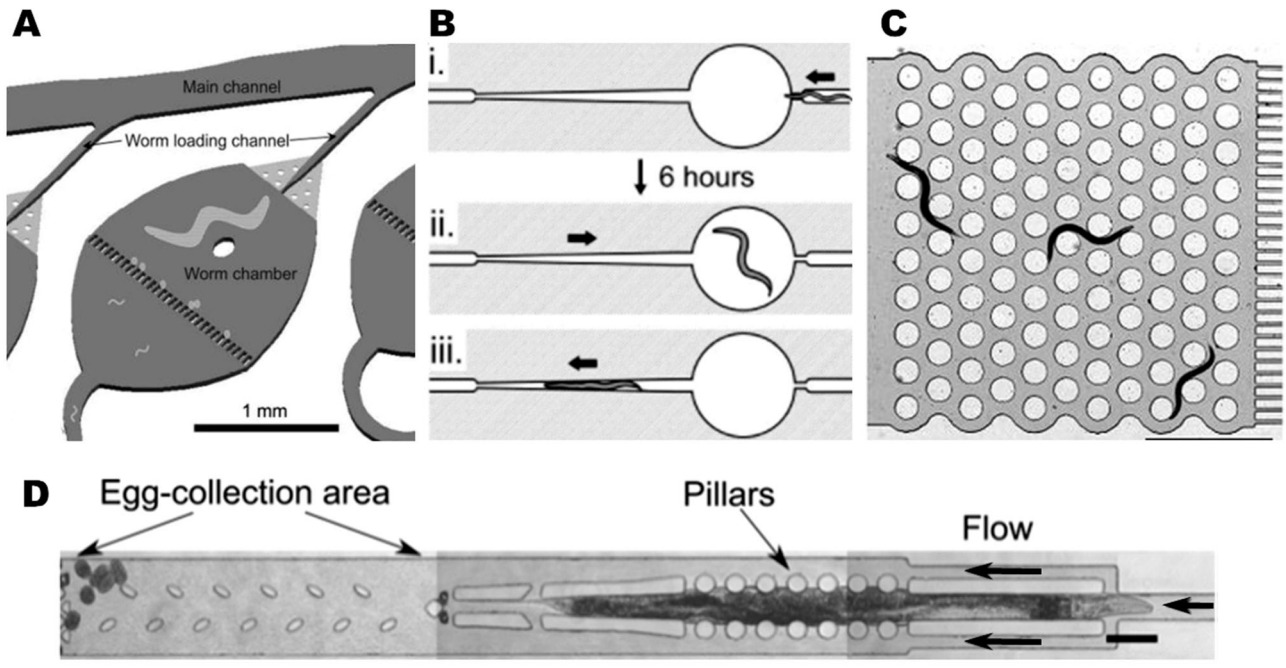

Figure 4. Longitudinal Imaging. (A) A worm chamber with a progeny filter (Li et al. 2015). Progenies are flushed out while the adult worm remains trapped. (B) A worm chamber with a tapered channel for immobilization (Hulme et al. 2010). Worms are pushed into the tapered channel for imaging. (C) Artificial dirt allows crawling of worms in a liquid environment (Larsch et al. 2013). (D) 'WormSpa' developed by Kopito and Levine (2014). Microstructures and flow keep a worm confined in an individual imaging chamber. Eggs laid are collected due to another microstructure on the left. The images were reproduced from Li et al. (2015), Hulme et al. (2010), and Kopito and Levine (2014) with permission from the Royal Society of Chemistry and Larsch et al. (2013). (Copyright (2013) National Academy of Sciences).

pattern, allowing worms to crawl as if they are on dirt, despite the liquid environment on the chip. Artificial dirt enabled the behavioural analysis of worms in a precisely controlled environment with superb imaging quality compared to that on agar plates (Albrecht and Bargmann 2011); high-throughput imaging of neuronal activity in response to odors and pharmacological stimuli (Larsch et al. 2013); study of the effects of *Pseudomonas* infection on survival, gene expression, motility, and the bacterial colonization of the intestine (Lee et al. 2016); and more. While these assays were not longitudinal, and examined more than 10 worms in a bigger arena, Banse *et al.* demonstrated another chip with an array of single-worm artificial-dirt arenas and analyzed their response to dietary, osmotic, and oxidative stress (Banse et al. 2019)

An alternative approach to provide a friendly environment for worms in a microfluidic chip is to keep each individual in a small confinement while allowing head movements, egg-laying, and small back-and-forth motion, similar to worms that are 'dwelling' on a plate (Arous et al. 2009). In a microfluidic chip termed 'WormSpa' (Figure 4(D)), worms exhibit fast pharyngeal pumping motion, lay many eggs, and do not actively move around, just like the worms on agar plates with abundant food resources (Kopito and Levine 2014; Lee et al. 2017; Lee and Levine 2018).

The embryo incubator chip (Cornaglia et al. 2015) mentioned above (Figure 2(B)) is also a longitudinal imaging technique that enables monitoring the development of an individual embryo separately. As an alternative to microfluidics-based approaches, Gritti *et al*. developed a novel method to confine a single larva in a microchamber with a bacterial lawn on a solid surface (Gritti et al. 2016). They ensured that each larva does not leave its own lawn by covering the chambers with a polyacrylamide hydrogel.

Other useful components

Novel experimental approaches on microfluidic chips are consistently being developed, and many interesting features enable advanced manipulation of worms and precise control of experimental conditions that are not available otherwise. In Figure 5, several of such useful features for microfluidic devices are introduced.

Figure 5(A) shows the operating principle of how to produce a droplet in a microfluidic device (Aubry et al. 2015). A droplet is formed at a four-way junction, where short pulses of worms in pluronic solution,

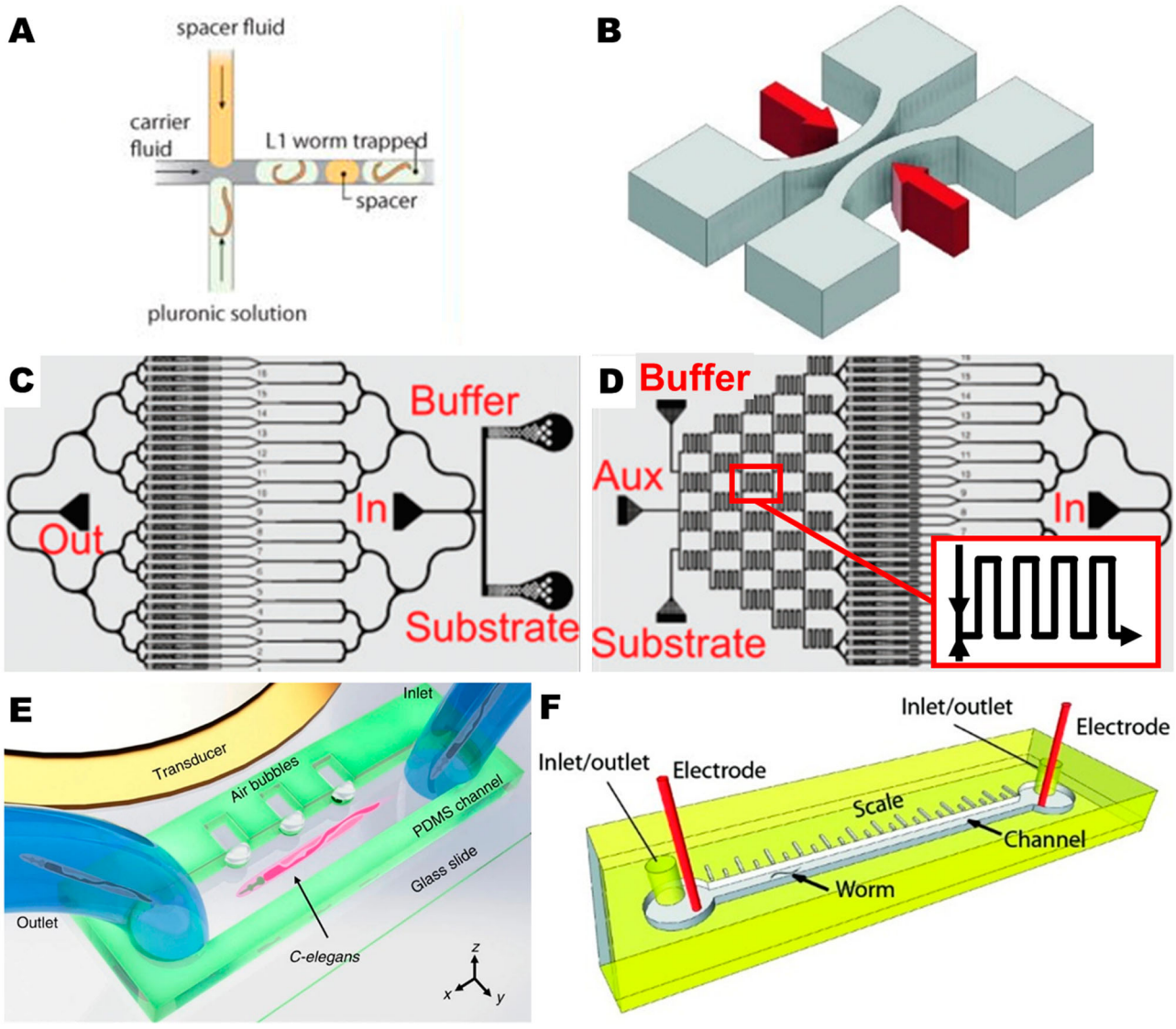

Figure 5. Other interesting components. (A) The working principle of droplet generation in a four-way junction. Droplets of pluronic solution trapping a larva are separated by droplets of space fluid (Aubry et al. 2015). (B) A microfluidic chip for studying mechanical stimuli developed by Cho et al. (2017). Expanding control chambers exert pressure onto the flow chamber in the middle. (C) Environmental switching between buffer and substrate (Kopito and Levine 2014). (D) Concentration gradient created by cascades of 'zig-zag' components (Kopito and Levine 2014). (E) Acoustic manipulation of worms (Ahmed et al. 2016). Air bubbles trapped in the PDMS channel (green) oscillate due to the acoustic waves from the transducer (yellow) to generate microvortices in the channel, which manipulate the worm (magenta). (F) Electrodes in a microfluidic chip induce electrotaxis of worms (Salam et al. 2013). The images were reproduced from Aubry et al. (2015) and Kopito and Levine (2014) with permission from the Royal Society of Chemistry, Cho et al. (2017) with permission under the terms of the Creative Commons Attribution 3.0 Unported License (https://creativecommons.org/licenses/by/3.0/), and Ahmed et al. (2016) and Salam et al. (2013) with permission under the terms of the Creative Commons Attribution Non-Commercial License (http://creativecommons.org/licenses/by-nc/4.0).

carrier fluid (silicone oil), and spacer fluid (FC-70 oil) enter sequentially to produce a series of droplets, each containing a single worm, and spacer droplets in a stream of carrier fluid. Worms encapsulated in droplets are better suited for high-resolution imaging and sorting.

Cho *et al.* developed a fully automated platform where a broad range of mechanical stimuli can be precisely applied to worms (Cho et al. 2017). Figure 5(B) illustrates the working principle of this chip, which is similar to pressurized valves (Figure 2), except that here pressure is applied horizontally rather than vertically. Worms immobilized in the middle channel are pushed from both sides as the pressure in the left- and right-side channel increases. This device was used to examine the effects of a wide range of mechanical pressures (from 15 to 60 psi) on worm size (Cho, Porto, et al. 2017).

The fabrication techniques used to fabricate a layer of PDMS for a microfluidic chip can also be applied to fabricate a PDMS mold for printing an agar chip. Lee *et al.* developed the 'micro-dirt' chip, a device made of agar designed to mimic a natural soil environment with repeated arrays of micro-posts (Lee et al. 2011). Using this device, they could quantify the nictation behaviour of worm and revealed that nictation is a dispersal behaviour regulated by IL2 neurons (Lee et al. 2011).

Capability to control the environment precisely and rapidly is one of the many benefits of microfluidic devices. Figure 5(C) shows an example of implementation of environmental switching in a microfluidic chip (Kopito and Levine 2014). In an experiment in which the response of the animals to stimuli or the removal of the stimuli is examined, the buffer solution in the chip must be replaced with the substrate solution, or vice versa. To do so, the device is connected to the reservoirs of the buffer and the substrate solution via the two inlets on the right (Figure 5(C)), but only one solution is injected into the chip at any given time. As soon as the solution being injected is changed from one to the other, the liquid in the chip is replaced and the environment is switched. This component can be connected to various microfluidic devices to add the environmental switching capability. A similar principle is used in devices designed to study olfaction, where two additional channels with dyes of different colours are used to visualize which solution is filling the chamber (Chronis et al. 2007). A somewhat more complicated design is used to mix two solutions at a gradient of concentrations (Figure 5(D)) (Kopito and Levine 2014). Two solutions passing through the zig-zag path (Figure 5(D) inset) come out very well mixed. By cascading these zig-zag mixers, the buffer solution and the substrate solution are mixed to eight channels of different concentrations (Figure 5(D)). An auxiliary inlet determines the concentration profile of the eight channels: for example, a linear profile across the eight channels was achieved when a concentration of 50% was injected at the auxiliary inlet.

Both acoustic and electric fields have been used to move worms. A microfluidic device developed by Ahmed *et al.* employs acoustic waves for rotational manipulation of worms (Figure 5(E)) (Ahmed et al. 2016). Air bubbles in an acoustic field oscillate to generate microvortices, and these vortices rotate the worm in a chamber to enable imaging of the worm at various angles. This technique requires a piezoelectric transducer that generates acoustic waves and air bubbles trapped in a chamber. A different device is based on electrotaxis, the tendency of worms to move in the direction of an electric field (Rezai et al. 2010). Introduction of electrodes into microfluidic chips, as in Figure 5(F), allows induction of locomotion in a favoured direction as well as sorting worms at different developmental stages (Han et al. 2012) or worms with defects in their nervous system (Salam et al. 2013).

Conclusion

As it has been almost 20 years since microfluidic devices were introduced to worm biology, the microfluidic technology has significantly improved and is capable of various complicated tasks. The trend seems to be heading towards increasing the throughput of experiments more and more for high content data, and high throughput sorting and screening (Mondal et al. 2016; Cho, Zhao, et al. 2017; Cornaglia et al. 2017; Midkiff and San-Miguel 2019). In an effort to develop such high throughput applications, experiments are becoming fully automated, and these advanced assays could require the support of robotics (Cornaglia et al. 2016) and sophisticated image analysis (Larsch et al. 2013; Kato et al. 2015).

Parallel with the increase in the sophistication of these devices, it has also become very difficult to adapt for novice users who are not familiar with microfluidics. To help with onboarding it is useful to understand that new devices are usually built on top of existing modules. It is therefore helpful to look at the basic building blocks of these highly advanced devices, and mix and match them for a desired application. Here, we reviewed various control components that are widely employed in the design of microfluidic devices. We discussed the flow-controlled (Figure 1) and pressure-controlled (Figure 2) immobilization methods. The components that can be considered for sorting worms at various developmental stages were also explained (Figure 3). We then looked into the different implementations for longitudinal imaging of worms (Figure 4). Finally, other interesting and useful applications were covered (Figure 5). We hope that understanding the basic elements of microfluidic chips will allow researchers who are new to microfluidics to design their own applications and will promote the invention of novel microfluidic chips in the future.

Acknowledgements

This research was supported by the NRF of Korea grant 2018R1A4A1024506 and 2019R1C1C1007124.

Disclosure statement

No potential conflict of interest was reported by the author(s).

Funding

This work was supported by National Research Foundation of Korea [grant numbers 2018R1A4A1024506, 2019R1C1C1007124].

ORCID

Kyung Suk Lee http://orcid.org/0000-0003-4157-5153

References

Ahmed D, Ozcelik A, Bojanala N, Nama N, Upadhyay A, Chen Y, Hanna-Rose W, Huang TJ. 2016. Rotational manipulation of single cells and organisms using acoustic waves. Nat Commun. 7:11085. eng.

Ai X, Zhuo W, Liang Q, McGrath PT, Lu H. 2014. A high-throughput device for size based separation of *C. elegans* developmental stages. Lab Chip. 14(10):1746–1752. eng.

Albrecht DR, Bargmann CI. 2011. High-content behavioral analysis of *Caenorhabditis elegans* in precise spatiotemporal chemical environments. Nat Methods. 8(7):599–605. eng.

Arous JB, Laffont S, Chatenay D. 2009. Molecular and sensory basis of a food related two-state behavior in *C. elegans*. PLoS One. 4(10):e7584–e7584. eng.

Aubry G, Zhan M, Lu H. 2015. Hydrogel-droplet microfluidic platform for high-resolution imaging and sorting of early larval *Caenorhabditis elegans*. Lab Chip. 15(6):1424–1431. eng.

Banse SA, Blue BW, Robinson KJ, Jarrett CM, Phillips PC. 2019. The stress-chip: a microfluidic platform for stress analysis in *Caenorhabditis elegans*. PLoS One. 14(5):e0216283. eng.

Casadevall i Solvas X, Geier FM, Leroi AM, Bundy JG, Edel JB, DeMello AJ. 2011. High-throughput age synchronisation of *Caenorhabditis elegans*. Chem Commun. 47(35):9801–9803. eng.

Cho Y, Porto DA, Hwang H, Grundy LJ, Schafer WR, Lu H. 2017. Automated and controlled mechanical stimulation and functional imaging in vivo in *C. elegans*. Lab Chip. 17 (15):2609–2618. eng.

Cho Y, Zhao CL, Lu H. 2017. Trends in high-throughput and functional neuroimaging in *Caenorhabditis elegans*. Wiley Interdiscipl Rev Syst Biol Med. 9:3. eng.

Chokshi TV, Ben-Yakar A, Chronis N. 2009. CO_2 and compressive immobilization of *C. elegans* on-chip. Lab Chip. 9 (1):151–157. eng.

Chronis N, Zimmer M, Bargmann CI. 2007. Microfluidics for in vivo imaging of neuronal and behavioral activity in *Caenorhabditis elegans*. Nat Methods. 4(9):727–731. eng.

Chung K, Crane MM, Lu H. 2008. Automated on-chip rapid microscopy, phenotyping and sorting of *C. elegans*. Nat Methods. 5(7):637–643. eng.

Cornaglia M, Krishnamani G, Mouchiroud L, Sorrentino V, Lehnert T, Auwerx J, Gijs MA. 2016. Automated longitudinal monitoring of in vivo protein aggregation in neurodegenerative disease *C. elegans* models. Mol Neurodegener. 11:17. eng.

Cornaglia M, Lehnert T, Gijs MAM. 2017. Microfluidic systems for high-throughput and high-content screening using the nematode *Caenorhabditis elegans*. Lab Chip. 17(22):3736–3759. eng.

Cornaglia M, Mouchiroud L, Marette A, Narasimhan S, Lehnert T, Jovaisaite V, Auwerx J, Gijs MAM. 2015. An automated microfluidic platform for *C. elegans* embryo arraying, phenotyping, and long-term live imaging. Sci Rep. 5(1):10192.

Gokce SK, Guo SX, Ghorashian N, Everett WN, Jarrell T, Kottek A, Bovik AC, Ben-Yakar A. 2014. A fully automated microfluidic femtosecond laser axotomy platform for nerve regeneration studies in *C. elegans*. PLoS One. 9(12):e113917. eng.

Gritti N, Kienle S, Filina O, van Zon JS. 2016. Long-term time-lapse microscopy of *C. elegans* post-embryonic development. Nat Commun. 7(1):12500.

Han B, Kim D, Hyun Ko U, Shin JH. 2012. A sorting strategy for *C. elegans* based on size-dependent motility and electrotaxis in a micro-structured channel. Lab Chip. 12(20):4128–4134.

Hu C, Dillon J, Kearn J, Murray C, O'Connor V, Holden-Dye L, Morgan H. 2013. Neurochip: a microfluidic electrophysiological device for genetic and chemical biology screening of *Caenorhabditis elegans* adult and larvae. PloS One. 8(5): e64297. eng.

Hulme SE, Shevkoplyas SS, Apfeld J, Fontana W, Whitesides GM. 2007. A microfabricated array of clamps for immobilizing and imaging *C. elegans*. Lab Chip. 7(11):1515–1523. eng.

Hulme SE, Shevkoplyas SS, McGuigan AP, Apfeld J, Fontana W, Whitesides GM. 2010. Lifespan-on-a-chip: microfluidic chambers for performing lifelong observation of *C. elegans*. Lab Chip. 10(5):589–597. eng.

Hwang H, Barnes DE, Matsunaga Y, Benian GM, Ono S, Lu H. 2016. Muscle contraction phenotypic analysis enabled by optogenetics reveals functional relationships of sarcomere components in *Caenorhabditis elegans*. Sci Rep. 6:19900. eng.

Ide C, Valmas N, Hilliard MA, Lu H. 2012. Laterally orienting *C. elegans* using geometry at microscale for high-throughput visual screens in neurodegeneration and neuronal development studies. PLoS One. 7(4):e35037. eng.

Kamili F, Lu H. 2018. Recent advances and trends in microfluidic platforms for *C. elegans* biological assays. Annual review of analytical chemistry (Palo Alto. Calif. 11(1):245–264. eng.

Kato S, Kaplan Harris S, Schrödel T, Skora S, Lindsay Theodore H, Yemini E, Lockery S, Zimmer M. 2015. Global brain dynamics embed the motor command sequence of *Caenorhabditis elegans*. Cell. 163(3):656–669.

Keil W, Kutscher LM, Shaham S, Siggia ED. 2017. Long-term high-resolution imaging of developing *C. elegans* larvae with microfluidics. Dev Cell. 40(2):202–214. eng.

Kopito RB, Levine E. 2014. Durable spatiotemporal surveillance of *Caenorhabditis elegans* response to environmental cues. Lab Chip. 14(4):764–770. eng.

Laranjeiro R, Harinath G, Hewitt JE, Hartman JH, Royal MA, Meyer JN, Vanapalli SA, Driscoll M. 2019. Swim exercise in *Caenorhabditis elegans* extends neuromuscular and gut healthspan, enhances learning ability, and protects against neurodegeneration. Proc Natl Acad Sci U S A. 116 (47):23829–23839.

Larsch J, Ventimiglia D, Bargmann C, Albrecht D. 2013. High-throughput imaging of neuronal activity in *Caenorhabditis elegans*. Proc Natl Acad Sci U S A. 110(45):E4266–E4273.

Lee H, Choi MK, Lee D, Kim HS, Hwang H, Kim H, Park S, Paik YK, Lee J. 2011. Nictation, a dispersal behavior of the nematode *Caenorhabditis elegans*, is regulated by IL2 neurons. Nat Neurosci. 15(1):107–112. eng.

Lee KS, Iwanir S, Kopito RB, Scholz M, Calarco JA, Biron D, Levine E. 2017. Serotonin-dependent kinetics of feeding bursts underlie a graded response to food availability in *C. elegans*. Nat Commun. 8(1):14221.

Lee H, Kim SA, Coakley S, Mugno P, Hammarlund M, Hilliard MA, Lu H. 2014. A multi-channel device for high-density target-selective stimulation and long-term monitoring of cells and subcellular features in *C. elegans*. Lab Chip. 14 (23):4513–4522. eng.

Lee KS, Lee LE, Levine E. 2016. HandKAchip – hands-free killing assay on a chip. Sci Rep. 6(1):35862.

Lee KS, Levine E. 2018. A microfluidic platform for longitudinal imaging in *Caenorhabditis elegans*. J Vis Exp. 135:57348. eng.

Li S, Stone HA, Murphy CT. 2015. A microfluidic device and automatic counting system for the study of *C. elegans* reproductive aging. Lab Chip. 15(2):524–531. eng.

Lockery SR, Hulme SE, Roberts WM, Robinson KJ, Laromaine A, Lindsay TH, Whitesides GM, Weeks JC. 2012. A microfluidic device for whole-animal drug screening using electrophysiological measures in the nematode *C. elegans*. Lab Chip. 12(12):2211–2220. eng.

Lockery SR, Lawton KJ, Doll JC, Faumont S, Coulthard SM, Thiele TR, Chronis N, McCormick KE, Goodman MB, Pruitt BL. 2008. Artificial dirt: microfluidic substrates for nematode neurobiology and behavior. J Neurophysiol. 99(6):3136–3143. eng.

Ma H, Jiang L, Shi W, Qin J, Lin B. 2009. A programmable microvalve-based microfluidic array for characterization of neurotoxin-induced responses of individual *C. elegans*. Biomicrofluidics. 3(4):44114. eng.

Midkiff D, San-Miguel A. 2019. Microfluidic technologies for high throughput screening through sorting and on-chip culture of *C. elegans*. Molecules. 24:23. eng.

Mondal S, Hegarty E, Martin C, Gökçe SK, Ghorashian N, Ben-Yakar A. 2016. Large-scale microfluidics providing high-resolution and high-throughput screening of *Caenorhabditis elegans* poly-glutamine aggregation model. Nat Commun. 7(1):13023.

Muthaiyan Shanmugam M, Subhra Santra T. 2016. Microfluidic devices in advanced *Caenorhabditis elegans* research. Molecules. 21:8. eng.

Rezai P, Salam S, Selvaganapathy PR, Gupta BP. 2012. Electrical sorting of *Caenorhabditis elegans*. Lab Chip. 12(10):1831–1840. eng.

Rezai P, Siddiqui A, Selvaganapathy PR, Gupta BP. 2010. Electrotaxis of *Caenorhabditis elegans* in a microfluidic environment. Lab Chip. 10(2):220–226. eng.

Rohde CB, Zeng F, Gonzalez-Rubio R, Angel M, Yanik MF. 2007. Microfluidic system for on-chip high-throughput whole-animal sorting and screening at subcellular resolution. Proc Natl Acad Sci U S A. 104(35):13891–13895. eng.

Salam S, Ansari A, Amon S, Rezai P, Selvaganapathy PR, Mishra RK, Gupta BP. 2013. A microfluidic phenotype analysis system reveals function of sensory and dopaminergic neuron signaling in *C. elegans* electrotactic swimming behavior. Worm. 2(2):e24558. eng.

Scholz M, Lynch DJ, Lee KS, Levine E, Biron D. 2016. A scalable method for automatically measuring pharyngeal pumping in *C. elegans*. J Neurosci Methods. 274:172–178.

Schrödel T, Prevedel R, Aumayr K, Zimmer M, Vaziri A. 2013. Brain-wide 3D imaging of neuronal activity in *Caenorhabditis elegans* with sculpted light. Nat Methods. 10 (10):1013–1020. eng.

Shi W, Wen H, Lu Y, Shi Y, Lin B, Qin J. 2010. Droplet microfluidics for characterizing the neurotoxin-induced responses in individual *Caenorhabditis elegans*. Lab Chip. 10(21):2855–2863. eng.

Sofela S, Sahloul S, Rafeie M, Kwon T, Han J, Warkiani ME, Song YA. 2018. High-throughput sorting of eggs for synchronization of *C. elegans* in a microfluidic spiral chip. Lab Chip. 18 (4):679–687. eng.

Stirman JN, Brauner M, Gottschalk A, Lu H. 2010. High-throughput study of synaptic transmission at the neuromuscular junction enabled by optogenetics and microfluidics. J Neurosci Methods. 191(1):90–93. eng.

Wang X, Tang L, Xia Y, Hu L, Feng X, Du W, Liu BF. 2013. Stress response of *Caenorhabditis elegans* induced by space crowding in a micro-column array chip. Integr Biol. 5(4):728–737. eng.

Yan Y, Ng LF, Ng LT, Choi KB, Gruber J, Bettiol AA, Thakor NV. 2014. A continuous-flow *C. elegans* sorting system with integrated optical fiber detection and laminar flow switching [10.1039/C4LC00494A]. Lab Chip. 14(20):4000–4006.

Youssef K, Tandon A, Rezai P. 2019. Studying Parkinson's disease using *Caenorhabditis elegans* models in microfluidic devices. Integr Biol. 11(5):186–207. eng.

Zhu G, Yin F, Wang L, Wei W, Jiang L, Qin J. 2016. Modeling type 2 diabetes-like hyperglycemia in *C. elegans* on a microdevice. Integr Biol. 8(1):30–38. eng.